

## HOLOGRAPHIC MEASUREMENT OF VELOCITY GRADIENTS IN FLUID FLOWS SENSITIZED WITH PHOTOCROMIC DYES

J. C. AGÜI and L. HESSELINK

Dept. Aeronautics & Astronautics  
 Stanford University  
 Stanford, CA 94305  
 USA

### Abstract

We present a novel joint application of holography and of photochromic materials to the measurement of velocity gradients in a fluid flow. A short study of photochromic materials of interest is presented from the point of view of their applicability to experimental fluid mechanics. The forced Rayleigh scattering method for measuring velocity gradients using photochromic materials is briefly described and applied to the measurement of the velocity gradient in a boundary layer. Spatial resolution up to  $100 \mu\text{m}$  and gradient resolution of  $3 \text{ s}^{-1}$  are obtained using these techniques.

### Introduction

The measurement of the vorticity in a fluid flow, both in a local region or over an extended area, is of interest in fluid mechanics research. However, the measurement of vorticity is difficult because, when compared with velocity measurements, it has much wider power distributions over the high temporal and spatial frequencies of the motion.

Customarily, vorticity data has been derived from velocity measurements. Since this approach requires the simultaneous measurement of velocity at different locations, it becomes very complex to apply and has limited spatial resolution. Furthermore, the difference operation commonly used to estimate vorticity generates fairly large errors, if a reasonable spatial resolution is attempted.

It is therefore highly desirable to perform single point measurements of vorticity or, alternatively, of velocity gradients. To that extent, a probe with a response to the gradients in the velocity across its measuring volume is required. Frish & Webb (1981) suspended particles with an imbedded reflector to provide a marker in the flow that is sensitive to the rotation of the flow. It is even more desirable to have a nonintrusive method that does not require the addition of solid macroscopic bodies inside the flow. Fermigier (1982), and Cloitre et al. (1986) have proposed and demonstrated a method using small plane thermal diffraction gratings for the measurements of velocity gradients. For their method it is only required to add an optically absorbing soluble dye to the working fluid. The distortion and rotation of the diffraction grating is related to the velocity gradient.

We present in this work a similar optical method that has advantages over the previous ones cited. We use volume, also called "thick", holograms as markers, and sensitize the flow with the addition of a photochromic dye. The advantages of this method are higher spatial resolution, and the ability of measuring much lower rotation rates. The new optical arrangement results in simpler accessibility requirements, and it can be shown that volume holograms lend themselves to a variety of alternate optical geometries for the measurement of different components of the tensor gradient.

### Description of the Method

The forced Rayleigh scattering (FRS) method essentially consists of a two step process. In the first one, a periodic variation of a physical property of the medium is written in it by optical means. In the second step, the evolution of that perturbed property is analyzed, again optically, by diffracting a beam from the evolving periodic perturbation of the material. An extensive survey of different uses of FRS methods is given by Eichler (1986).

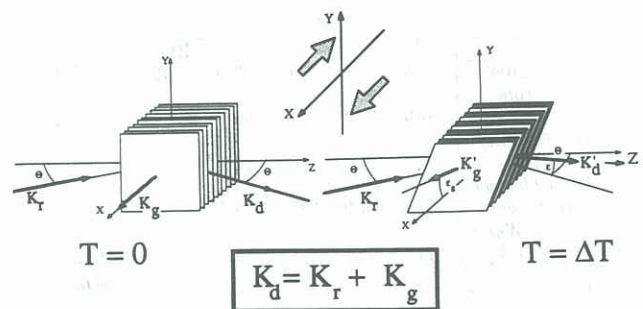


Figure 1: Schematic description of the Forced Rayleigh Scattering measurement of velocity gradients.

The application of FRS to the measurement of velocity gradients is also a two step process. First a periodic structure, i.e. a hologram, is written in the flow. This amounts to a selection of both, a measuring volume within the body of the fluid and, more important for this method, of a direction within the flow. This direction is defined by the normal to the planes of the fringes of the hologram. This hologram is written by the interference of two mutually coherent pulsed laser beams, like in LDV measurements, inside an absorbing material. This is shown in fig. 1. The pattern is impressed in the flow through the resulting local changes of the optical properties of the fluid. These changes are proportional to the intensity of the radiation pattern at each point. The writing of the hologram takes place in times much shorter than any time scale of the flow. The orientation of the hologram can be, at any time, probed by diffracting a beam from it. The vector describing the direction of the diffracted light is obtained by vector summation of the wave vector associated with the reading beam and the vector normal to the plane of the fringes, as shown in fig. 1.

After the hologram is written in the fluid, the motion of the fluid flow acts on it. A uniform velocity simply translates it to a different position, while a non uniform velocity results in both a translation and a net rotation. The second step is now to constantly monitor the new orientation of the marker by measuring changes in the direction of the diffracted beam. This process is carried out for long enough time so that a linear rotation time can be fitted or, ultimately, until the diffracted beam decays because of diffusion of the hologram or other effects. The method is therefore insensitive to the mean transport velocity of the hologram.

## Photochromic Materials

The addition of photochromic dyes to the working fluid makes it possible to record the hologram in it. Though just thermal gratings could be used by adding non photochromic absorbing dyes, the photochromic mechanism permits longer lived holograms. The mass diffusivity coefficient is two orders of magnitude smaller than for heat. So the diffusion process—which is responsible for the decay of the hologram—is much slower for photochromic than for thermal holograms.

Photochromism consists of a reversible change in the optical properties of materials when irradiated with light of the proper wavelength. The absorption of one or more photons produces a morphological change in the molecule which results in a change of its optical properties. This change is reflected in variations of the absorption and index of refraction spectra. In most cases the modified molecules will revert to the original, more stable form, if left for some time in the dark. This back reaction can also be excited with radiation of the appropriate wavelength.

Photochromic materials have been used in experimental fluid mechanics (see the work of Kondratas (1980), and Dembek (1980)). These materials are not however, suitable for FRS measurements, since they need ultraviolet light to be turned from their stable transparent form into the colored one. Furthermore, they are only soluble in organic solvents, which presents some experimental difficulties. Table 1 contains a list of properties of interest for some of the most important photochromic materials.

	$\lambda_c$	$\alpha_c$	$\lambda_{nc}$	$\alpha_{nc}$	Ret.	$\phi$
6-N-Bips <i>Toluene</i>	598	5.9	*340	2.6	59	$\approx 1$
8-N-Bips <i>H<sub>2</sub>O-p-diox.</i>	*540	4.14	430	0.69	$\geq 5$	0.5
Hg(Dz) <sub>2</sub> <i>Chloroph.</i>	600	9.7	*480	17.1	4	
M. Green <i>Water</i>	625	15.9	*275	9.1		0.9
ThioIndigo <i>Toluene</i>	*542	4.1	*485	3.1		(.26) <sub>et</sub> (.03) <sub>tc</sub>

Table 1: Photochromic properties of some characteristic photochromic materials. The \* symbol denotes the stable form in dark (both forms of Thioindigo are simultaneously present under these conditions). Subindices *c* and *nc* stand for the "colored" and the "non-colored". They correspond to the molecule states having the peak absorption at the longest and shortest wavelength, respectively. "Ret." is the characteristic time for the thermally induced backreaction, from the excited to the stable form.  $\phi$  is the quantum efficiency of the coloration reaction. Absorption coefficients are expressed in  $\times 10^4 \text{ cm}^{-1} (\text{mol/l})^{-1}$ . Wavelengths in nm.

During this work we have found an alternate photochromic material that shows promising features for its non visualization use. 8-Nitro-Bips is, in mixtures of water and p-dioxane, stable in its colored form, and shows photochromic behavior at visible wavelengths. Figure 2 shows the mechanism of that transformation. The molecule has two alternate forms, and molecules can be transferred from one to the other by light irradiation. The closed form is colorless, and is stable in the dark in non polar solvents. The open form absorbs in the green, and it is stable in a polar solvent. Ultraviolet radiation is necessary to convert an A-molecule into a B-molecule, while visible light can trigger the return from B to A. The equilibrium between the two forms is controlled by the polarity of the solvent. We have found that a solution of the dye in a mixture of water and p-dioxane with a 0.9 molar fraction of water has an absorption peak close to 520 nm, an that it can be efficiently bleached into a transparent form by irradiating it with a doubled Nd:YAG laser (532 nm). The recovery time, or the time needed for the unstable form to revert to the more stable one in darkness, is of the order of minutes, much longer than any other time involved. The concentration of dye required is small, of the order of  $10^{-4}$  mol/l.

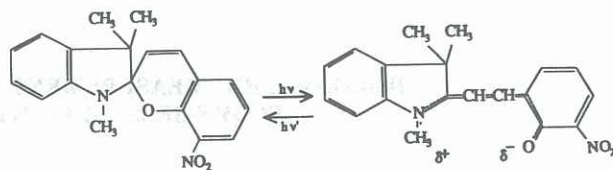


Figure 2: Photochromic mechanism of 8-nitro-BIPS. Left: Closed colorless form. Right: Open colored form.

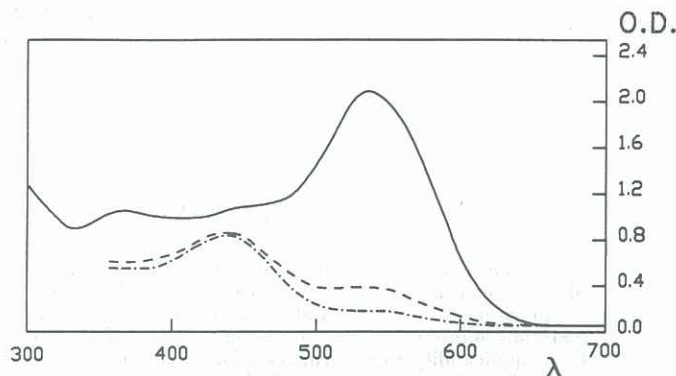


Figure 3: Absorption spectrum of the reverse photochromism of 8-nitro-BIPS  $10^{-4}$  mol/l in water-dioxane solution ( $\chi_{H_2O} = 0.9$ ). Solid: colored form (Stable). Dot-dashed: transparent form, immediately after bleaching. Dashed: 1 minute after bleaching.

Figure 3 contains the absorption spectrum of this material. More recent work has shown that solutions of 8-nitro-BIPS in mixtures of water and DMSO (dimethylsulphoxide) have similar photochromic behavior, and are less toxic than the water-dioxane mixtures.

We have also studied the writing of the hologram, or how the laser beam progress through the absorbing media till it reaches the interference point (see Agüí and Hesselink (1990)). The results show an optimum value for the concentration of the dye that maximizes the optical difference between peaks and valleys of the fringes in the hologram. It can also be shown that the optimum wavelength at which to read the hologram with maximum efficiency does not correspond to the peak of the absorption, but that it depends on the dye concentration and is generally in the wings of the absorption profile, in the red region of the spectrum. This is very convenient, since a He-Ne laser can then be used for continuously reading the hologram.

## Experimental Set up

A simplified version of the experimental optical set-up is contained in fig. 4. It consists of a laser source, a Quanta-Ray DCR2-10 Nd:YAG, whose output is split and focused onto the target volume by a lens. The pulse length of the laser limits the exposure time to a value of close to 30 ns. A 10 mW He-Ne laser is used for reading out the holograms, and its beam is focused on the target volume at the proper Bragg angle by reflection off a high-pass dichroic filter. Special care is also taken in the layout of the beam paths to ensure that both have the same optical length, to maintain the coherence necessary between the two interfering writing beams. Energy levels of approximately 5 mJ per pulse of 532 nm radiation over a 100 to 200  $\mu\text{m}$  diameter spot have been used for this work.

The diffracted beam of light is isolated from the undeflected writing and reading beams using a set of diaphragms and optical filters. The angular motion of the diffracted beam is converted into a displacement parallel to itself by a lens placed at a distance equal to its focal length from the measuring volume. This linear shift is measured with an EG&G Reticon CCD linear detector array.

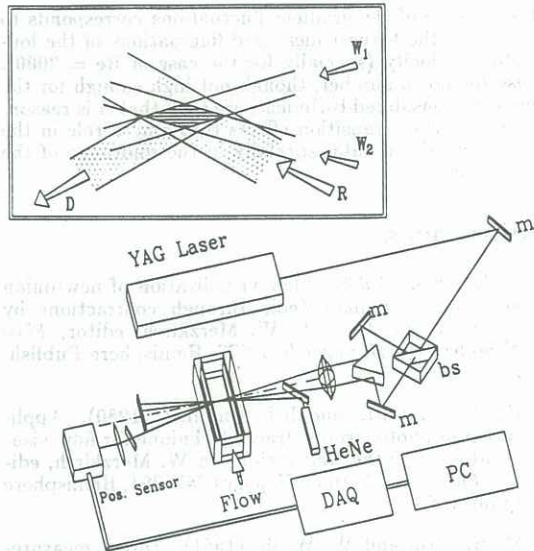


Figure 4: Experimental set-up. Box contains detail of the measuring volume. Hologram is written by beams  $W_1$  and  $W_2$ , and read by beam  $R$ . The diffracted beam,  $D$ , steers out of the plane of the writing and reading beams because of the rotation of the hologram around the optical axis.

The array is used in a constant scan mode, clocked at a frequency of 2 MHz, and provides a scan of the intensity profile of the diffracted spot approximately every 0.5 milliseconds. The output from the CCD array is recorded by a CAMAC-based Lecroy transient digitizing system, synchronized with the CCD array. The digitized data are uploaded to a computer workstation for analysis and display.

A small water tunnel has been built for this experiment, with a rectangular test section of 0.4 by 0.9 inches across and 5 inches long. It is entirely made of plexiglas except for two optically flat windows placed at the test section. Honeycomb and foam are used as flow straighteners and turbulence dampers, preceding a one-to-five contraction that leads to the test section.

## Experimental Results

The working fluid is a mixture of water and p-dioxane (molecular fraction of water,  $\chi_{H_2O} = 0.9$ ), and the photochromic dye is 8-nitro-BIPS at a concentration value of  $3 \times 10^{-4}$  mol/l. The optical arrangement is displayed in fig. 4. The cross section of the reading beam is typically around 0.5 mm, large enough to accommodate the shift in position that the hologram suffers during the measuring period. The fringe spacing within the hologram is determined by the wavelength and the intersection angle between the two writing beams. Small fringe spacings produce high efficiency holograms, but also result in short-lived holograms, since the effect of diffusion is then more pronounced. Consequently, the grating is made as small as possible for the range of the gradients to be measured, and a minimum number of 10 to 20 fringes per hologram is always kept. For the experimental results shown below, the spacing used is approximately  $24 \mu\text{m}$  and  $12 \mu\text{m}$ , for the channel and the boundary layer measurements, respectively. They result in diffusion-limited lifetimes of 20 and 5 ms.

The diffracted spot is isolated from the other beams and a vertical intensity profile through its middle point is recorded with the CCD array. The acquisition of the profiles is continued for the time period corresponding to the diffraction life of the hologram, thus obtaining the maximum number of scans possible. The digital processing of the scan data consists of estimating the center of gravity of the spot profile at each time and then fitting a linear curve to the translation of the position of that center of gravity as a function of time. That value is then related to the rotation rate of the hologram through a constant which depends solely on the experimental geometry. See Agüí & Hesslink (1988) for more details.

## Channel flow measurements

Figure 5 contains a profile of the gradient of the downstream velocity with respect to the normal coordinate running across the short dimension of the test section. The profile is taken from the center of the section to the wall along the same direction. The Reynolds number of the flow, based on the equivalent diameter of the cross section and the average velocity is 440. Downstream position  $X/D$  is 2.7. At these parameter settings, the flow is in a nearly fully developed condition for a rectangular cross section. The measuring volume for the data, *i.e.* the overlapping region of the two writing beams, is, for the data in fig. 5, an ellipsoid of 0.2 by 0.2 by 5 mm approximately, where the long dimension is aligned along the optical axis (right to left in fig. 4), parallel to the lower wall and perpendicular to the mean flow. The first point in fig. 5 is situated at just  $350 \mu\text{m}$  from the boundary of the flow. An estimate of the variability of the holographic measurements is obtained by acquiring a sufficiently large number ( $\geq 30$ ) of data points at each station and computing the mean and the standard deviation of the results. The mean value is considered to be the overall best measurement of the velocity gradient. The standard deviation is a measure of the uncertainty of the method. These values are correlated in fig. 5 with those obtained by finite-differencing an LDA-based velocity profile. Their agreement is within 5–10% for most data points. There is no available estimate of the uncertainty of the LDA based measurements.

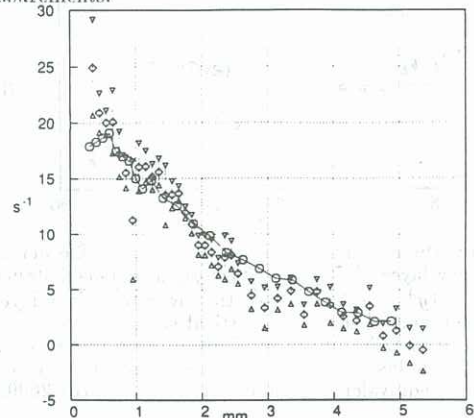


Figure 5: Gradient profile across the short span of the water tunnel. Reynolds number is 440.  $\circ$  and line: gradients as derived from LDA measurements.  $\diamond$ : gradients measured using holographic methods and associated estimated error. Center of the tunnel is located at 5.08 mm from the wall.

## Boundary layer measurements

Holographic measurements of the  $\partial u / \partial y$  gradient (where  $u$  is the downstream velocity and  $y$  is the distance normal to the lower wall) are contained in figs. 6 and are made dimensionless with the extrapolated value at the wall. The Reynolds number based on the flux velocity and the equivalent diameter of the cross section are 1500 and 2000 for figs. 6a and 6b, respectively. Table 2 lists the most relevant characteristics of the boundary layer flow measured.

The measuring volume is now an ellipsoid of 90 by 90 by  $1200 \mu\text{m}$ , with the longest dimension parallel to the wall and perpendicular to the mean flow. This reduced cross section is obtained by using a shorter focal length as the focusing lens, while the longer dimension is a result of the small angle between the interfering beams which is needed to make holograms that last for a reasonable time ( $\geq 1$  ms).

The reduced cross section of the measuring volume permits measurements at  $y^+$  values of order unity and to obtain accurate instantaneous values of the stresses very near to the wall ( $y \approx 100 \mu\text{m}$ ), where differentiation of velocity profiles is not possible because of the lack of spatial resolution of the velocity measuring methods. The data displayed in figs. 6 are an average of up to 32 measurements at each location, taken at the laser pulse rate of 10 Hz. The segments across each value show the fluctuations found in the measured values.

	(a)	(b)	
$U_\infty$	160	209	mm/s
$Re$	1500	2000	
$\delta_d$	0.87	0.73	mm
$Re_{\delta_d}$	135	148	
$Re_\delta$	428	469	
$u^*$	11.5	14.2	mm/s

Table 2: Summary of the properties of the boundary layers measured. Unsubscripted  $Re$  is based on the flux velocity and the equivalent diameter of the tunnel cross section.  $\delta_d$  and  $\delta$  represent the displacement and the  $0.99U_\infty$  thicknesses of the boundary layer. (a) and (b) correspond to the flow conditions of the data in figs. 6.

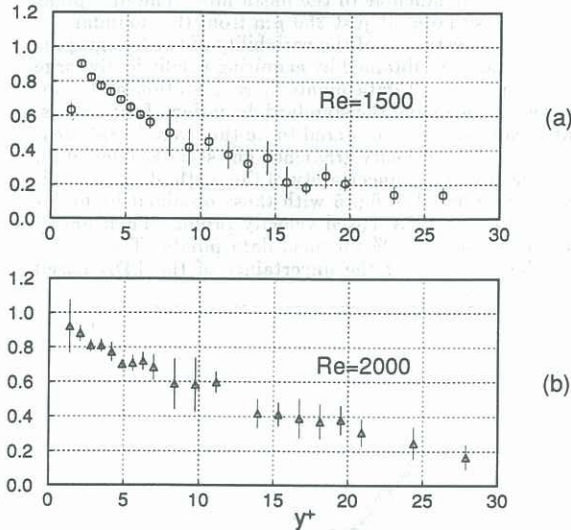


Figure 6: Dimensionless velocity gradient profile across a boundary layer.  $((\partial u/\partial y)/(\partial u/\partial y)_{y=0})$  versus distance to the wall ( $y^+ = yu^*/\nu$ ) across the lower boundary layer in the rectangular channel. Vertical segments show the estimated variability of the gradient at the corresponding station. Reynolds numbers based on the flux velocity and the channel equivalent diameter are: (a) 1500, (b) 2000.

## Discussion of the results

Figure 5 shows the accuracy of the holographic method and the expected level of noise present in the results. The minimum error of the method can be expected to be about  $2$  to  $3 \text{ s}^{-1}$ , which is the typical variability obtained in the results at low Reynolds numbers.

An important feature of these measurements is the range of the measurable values of the gradient, which is extended to very low values ( $\geq 3 \text{ s}^{-1}$ ). This is a direct result of the use of a photochromic material as the sensitizing agent in the flow, which produces longer-lived holograms than those achieved using thermal gratings.

Additionally, the use of photochromic materials permits high spatial resolutions. The very small cross section of the measuring volume in the downstream direction and in the direction perpendicular to the wall ( $200 \mu\text{m}$  in fig. 5;  $95 \mu\text{m}$  in figs. 6) allows measurements of the velocity gradient to be obtained as close to the wall as  $100 \mu\text{m}$ . Moreover, because of the single point nature of this measurement, the spatial resolution is limited only by the size of the measuring volume, and not by the physical spacing of the various probes required by other velocity based techniques.

The very low values of  $y^+$  of the measurements in figs. 6 should be, however, considered in conjunction with a rather low Reynolds number based on the core velocity and the displacement thickness ( $Re_{\delta_d}$ ) previously mentioned. The variability of the data, as expressed by the vertical bars in fig. 6, is rather small close to the wall, except for the nearest point at  $100 \mu\text{m}$  from it, and increases far from it, reaching its maximum at  $y^+ \approx 6 - 9$ .

This increase of the gradient fluctuations corresponds to the zone of the highest measured fluctuations of the longitudinal velocity (specially for the case of  $Re = 2000$ ). These Reynolds number, though not high enough for the flow to be considered turbulent, are such that it is reasonable to consider transition effects that play a role in the fluctuation of the data, specially in the midrange of the  $y^+$  studied.

## References

- [1] G. Dembek. (1980). Flow visualization of newtonian and non-newtonian media through contractions by photochromic dyes. In W. Merzkirch, editor, *Flow Visualization II*, pages 573-577, Hemisphere Publish. Co.
- [2] H. M. Kondratas and R.L. Hummel. (1980). Application of photochromic tracer technique for flow visualization near the wall region. In W. Merzkirch, editor, *Flow Visualization II*, pages 387-391, Hemisphere Publish. Co.
- [3] M. B. Frish and W. Webb. (1981). Direct measurement of vorticity by optical probe. *J. Fluid Mech.*, 107:173-200.
- [4] M. Fermigier, M. Cloitre, E. Guyon, and P. Jenffer. (1982). Utilisation de la diffusion Rayleigh forcée à l'étude d'écoulements laminaires et turbulents. *Journal de Mécanique Théorique et appliquée*, 1(1):123-146.
- [5] M. Cloitre and E. Guyon. (1986). Forced Rayleigh scattering in turbulent plane poiseuille flows. part 1. study of the transverse velocity-gradient component. *J. Fluid Mech.*, 164:217-236.
- [6] H.J. Eichler, P. Günter, and D.W. Pohl. (1986). *Laser induced dynamic gratings*. Springer Verlag.
- [7] J.C. Agüí and L. Hesselink. (1988). Holograms in motion. I: The effect of fluid motion on volume holograms. II: The diffracting capabilities of strained holograms. *J. Opt. Soc. Am. A.*, 5(8). pag. 1287-1308.
- [8] J.C. Agüí and L. Hesselink. (1990). Application of holography to the measurement of velocity gradients in fluid flows sensitized with photochromic dyes. *Physics of Fluids A*. To appear.